Plant Physiology and Biochemistry 141 (2019) 431–445

Contents lists available at ScienceDirect

Plant Physiology and Biochemistry

journal homepage: www.elsevier.com/locate/plaphy

Research article

Isolation and characterization of *S*-Adenosylmethionine synthase gene from cucumber and responsive to abiotic stress

Mei-Wen He[a], Yu Wang[a], Jian-Qiang Wu[a], Sheng Shu[a,b], Jin Sun[a,b], Shi-Rong Guo[a,b,*]

[a] *Key Laboratory of Southern Vegetable Crop Genetic Improvement, Ministry of Agriculture, College of Horticulture, Nanjing Agricultural University, Nanjing, 210095, China*
[b] *Suqian Academy of Protected Horticulture, Nanjing Agricultural University, Suqian, 223800, China*

ARTICLE INFO

Keywords:
Cucumis sativus
S-adenosylmethionine synthetase
Gene expression
Function
Salt stress

ABSTRACT

S-adenosylmethionine synthetase (SAMS) catalyzes methionine and ATP to generate S-adenosyl-L-methionine (SAM). In plants, accumulating *SAMS* genes have been characterized and the majority of them are reported to participate in development and stress response. In this study, two putative *SAMS* genes (*CsSAMS1* and *CsSAMS2*) were identified in cucumber (*Cucumis Sativus* L.). They displayed 95% similarity and had a high identity with their homologous of *Arabidopsis thaliana* and *Nicotiana tabacum*. The qRT-PCR test showed that *CsSAMS1* was predominantly expressed in stem, male flower, and young fruit, whereas *CsSAMS2* was preferentially accumulated in stem and female flower. And they displayed differential expression profiles under stimuli, including NaCl, ABA, SA, MeJA, drought and low temperature. To elucidate the function of cucumber *SAMS*, the full-length CDS of *CsSAMS1* was cloned, and prokaryotic expression system and transgenic materials were constructed. Expressing CsSAMS1 in *Escherichia coli* BL21 (DE3) improved the growth of the engineered strain under salt stress. Overexpression of *CsSAMS1* significantly increased MDA content, H_2O_2 content, and POD activity in transgenic lines under non-stress condition. Under salt stress, however, the MDA content of transgenic lines was lower than that of the wild type, the H_2O_2 content remained high, the polyamine and ACC synthesis in transgenic lines exhibited a *CsSAMS1*-expressed dependent way. Taken together, our results suggested that both *CsSAMS1* and *CsSAMS2* were involved in plant development and stress response, and a proper increase of expression level of *CsSAMS1* in plants is benificial to improving salt tolerance.

1. Introduction

S-adenosylmethionine synthase (SAMS), containing the methionine binding site in the N-terminal domain and the ATP binding motif in the C-terminal, catalyzes the synthesis of S-adenosylmethionine (SAM) from methionine and ATP (Grillo and Colombatto, 2008; Markham and Pajares, 2009). It has been well known that SAM not only provides methyl groups for the methylation of DNA, RNA, proteins, and lipids but also participates in the synthesis of polyamines (PAs) and plant hormone ethylene (Roje, 2006; Burstenbinder et al., 2007). Plant PAs includes putrescine (Put), spermidine (Spd) and spermine (Spm). There are two pathways for the synthesis of Put from arginine, with either agmatine or ornithine as an intermediate. Put is converted into Spd and Spm by spermidine synthases (SPDS) and spermine synthase (SPMS) through the addition of aminopropyl groups from decarboxylated SAM, which is produced from SAM by *S*-adenosylmethionine decarboxylase (SAMDC). In plants, PAs have been implicated in regulating growth, development and stress responses (Kusano et al., 2008; Gupta et al., 2013; Minocha et al., 2014). The synthesis of ethylene begins with the conversion of methionine to SAM by the SAMS. SAM is converted to 1-aminocyclopropane-1-carboxylate (ACC) by ACC synthase (ACS) before ethylene is ultimately generated by ACC oxidase (Roeder et al., 2009). Ethylene is also involved in numerous plant physiological processes, such as plant development and signal transduction (Wang et al., 2002; Vandenbussche et al., 2012). As the common precursor of PAs and ethylene, SAM has been studied for its role in controlling plant development and stress response. Previous studies have confirmed that the biosynthesis of PAs could be inhibited by ethylene, and exogenous PAs could reduce ethylene emission (Bregoli et al., 2002; Li et al., 2013b). PAs and ethylene in some physiological processes might inhibit each other to maintain plants a favorable status.

The amino acid sequence of SAMS is fairly conserved during

---

[*] Corresponding author. Key Laboratory of Southern Vegetable Crop Genetic Improvement, Ministry of Agriculture, College of Horticulture, Nanjing Agricultural University, Nanjing, 210095, China.
E-mail address: srguo@njau.edu.cn (S.-R. Guo).

https://doi.org/10.1016/j.plaphy.2019.06.006
Received 22 April 2019; Received in revised form 12 May 2019; Accepted 6 June 2019

evolution, which implicates that the function of SAMS is considerably important. To date, genes encoding SAMS have been isolated from many plant species, such as Arabidopsis (Peleman et al., 1989), rice (Breusegem et al., 1994), tomato (Espartero et al., 1994), *Pinus contorta* (Lindroth et al., 2001), *Panax ginseng* (Pulla et al., 2009), Chinese cabbage (Yu et al., 2012), Brassica rapa (Kim et al., 2012), barley (Kim, 2013), *Lycoris radiata* (Li et al., 2013c), lotus (Quan et al., 2014), potato (Kim et al., 2015), soybean (Wang et al., 2016), and *Andropogon virginicus* (Ezaki et al., 2016). However, only the functions of SAMS in *Arabidopsis*, rice, Chinese cabbage, and tomato have been well explained. Both overexpression and silencing of *AtSAMS1* in tobacco resulted in abnormal phenotypes, high SAMS level producing coloration and flattening leaves, low SAMS content leading to asymmetric and torn leaves (Boerjan et al., 1994). One mutant of *AtSAMS3*, *mto3*, with a high level of free methionine, showed no visible growth difference but caused significantly decreased lignin content (Shen et al., 2002). RNA interference (RNAi) transgenic rice with repressed transcripts of all three *OsSAMS* led to dwarfism, delayed germination, reduced fertility, and late flowering phenotypes (Li et al., 2011). Transgenic Chinese cabbage plants overexpressing *SAMS* have been found to grow rapidly with flattened and serrated leaf margin, while down-regulated *SAMS* lines displayed stunted growth with thick and asymmetric leaves (Yu et al., 2012). In tomato, the expression of *SlSAMS* was enhanced by salt stress, and overexpression of *SlSAMS* increased tomato tolerance to alkali stress through PA metabolism (Sanchez-Aguayo et al., 2004; Gong et al., 2014). Until now, the knowledge of *SAMS* family members in Cucurbit crops is largely poor, and their functions have not been reported mainly due to the challenge in transgene technology.

Cucumber is one of the most important vegetables worldwide. However, biotic and abiotic stresses, such as pests, heat, salinity, and drought, cause great adverse effects on cucumber production and quality. Among them, cucumber is highly sensitive to salinity for its character of shallow-rooted, especially in early growth phases. Salinity inhibits nutrient uptake mainly due to the accumulation of Na^+, then affects a series of physiological processes, retards plant growth. The positive effects of exogenous PAs on salt stress tolerance in cucumber have been demonstrated in previous studies (Zhang et al., 2009; Shu et al., 2014; Yuan et al., 2017). Proteomics researches have revealed that exogenous PAs can alleviate salt injury by activating stress defense, enhancing expression of proteins involved in carbohydrate metabolism, and increasing K^+ uptake in cucumber (Li et al., 2013a; Yuan et al., 2016). However, the characterization and function analysis of PAs biosynthesis in cucumber are largely unknown.

In this study, two putative *SAMS* genes were identified in cucumber, designated as *CsSAMS1* and *CsSAMS2*. Sequence homology, gene structures, expression patterns in various organs were investigated. The expression profiles of the *CsSAMS1* and *CsSAMS2* under various stimuli were examined. In addition, we cloned the *CsSAMS1* from cucumber leaves and analyzed its impacts on the growth of engineered strain by expressing in *Escherichia coli* BL21 (DE3), and functions under salt stress by heterologous expression in tobacco. Our data suggest that *CsSAMS1* may be a potential candidate gene related to plant growth and stress response.

2. Materials and methods

2.1. Identification and sequence analysis of CsSAMS

To identify putative *SAMS* genes in cucumber, BLASTp searches of Cucumber Genome Database (http://cucumber.genomics.org.cn/page/cucumber/blast.jsp) were performed using the amino acid sequence of AtSAMSs. Then we checked the results in Cucurbit Genomics Database and NCBI Database. Amino acid sequences of cucumber SAMS proteins were aligned by BioXM (version 2.7) software. Meanwhile, the molecular weight and theoretical isoelectric point of the deduced polypeptides were calculated. Gene structure analysis was plotted using IBS (Liu et al., 2015). The phylogenetic tree was constructed using MEGA (version 6.0) with the neighbor-joining method (Saitou, 1987) and bootstrap analysis (1000 replicates). The SAMS proteins used in the phylogenetic relationship analysis was shown in Supplemental Table 1. Additionally, 1700 base pairs (bp) genomic sequences upstream of the initiation codon (indicated with +1) of cucumber SAMS genes were obtained and used for putative *cis*-elements prediction with the PantCARE (http://bioinformatics.psb.ugent.be/webtools/plantcare/html/).

2.2. Plants and treatments

Cucumber (*Cucumis sativus* L.) seedlings of an inbred line '9930' at the two-leaf stage grown in a hydroponic system were used to examine the gene expression patterns in different treatments. The containers (450 × 320 × 150 mm) containing half-strength Hoagland's nutrient solution (pH 6.5 ± 0.2, EC 2 ± 0.2 mS cm^{-1}) were jetted air using an electromagnetic air pump (ACO-006, Resun, Hangzhou, China) to maintain dissolved oxygen (DO) levels at 8.0 ± 0.2 mg L^{-1}, and the solutions were renewed every three days. At the three-leaf stage, plants were treated as follow, with 75 mM NaCl as salt stress, with 20% polyethylene glycol (PEG) 6000 as drought stress, with 4 °C as cold stress, spraying leaves with 100 μM salicylic acid (SA), 100 μM methyl jasmonate (MeJA), and 100 μM abscisic acid (ABA) as hormones treatment. The samples were collected at 0, 1, 2, 6, 12, and 24 h. All the samples were frozen immediately in liquid nitrogen and stored at −80 °C until used for RNA extraction.

2.3. Quantitative real-time PCR analysis

Total RNA was extracted with the RNA Simple Total RNA Kit (Tiangen, DP419) according to the manufacturer's instructions. Total RNA (1 μg) was used to synthesize cDNA template with the PrimeScript™ II 1st Strand cDNA Synthesis Kit (Takara, 6210A). The qRT-PCR tests were performed using the ChamQ Universal SYBR qPCR Master Mix (Vazyme, Q711-02) in a total volume of 20 μL, including 10 μL of SYBR qPCR Master Mix (2 ×), 2 μL of cDNA (diluted ten-fold), 0.8 μL of each specific primer, 0.4 μL of ROX reference dye and 6 μL of ddH_2O. The qPCR began with an initial denaturation at 95 °C for 10 s, followed by 40 cycles at 95 °C for 10 s, annealing at 60 °C for 30 s and extension at 72 °C for 30 s. The cucumber *ACTIN* gene was used as an internal control. Gene-specific primers designed according to cDNA sequences were listed in Supplemental Table 2. The relative gene expression levels were calculated with the $2_T^{-\Delta\Delta C}$ methods (Livak and Schmittgen, 2001).

2.4. Heterologous expression of CsSAMS1 in E. coli and growth in the presence of Na^+

The full-length CDS region of CsSAMS1 (1182 bp) amplified with primers pET-SAMS-F and pET-SAMS-R (Supplemental Table 2) was introduced into the pET-32a (+) expression vector. The resulting recombinant plasmid was then transformed into *Escherichia coli* BL21 (DE3) strain. Overnight cultures of BL21 (DE3)/pET-32a (+) and BL21 (DE3)/pET-32a-CsSAMS1 were adjusted to OD_{600} at 0.5 in 20 mL fresh LB medium before adding 0.1 mM IPTG. After the inoculation for 4 h at 28 °C, the OD_{600} value of BL21 (DE3)/pET-32a (+) and BL21 (DE3)/pET-32a-CsSAMS1 was 1.793 and 2.794, respectively. The OD_{600} value of their initial inoculation point (0 h) was 0.021 and 0.048, respectively. Next, 200 μL of induced cultures were transferred into 20 mL LB medium with 0, 200, 400, 600 mM NaCl, respectively. The cell density of the samples was detected at 1, 2, 3, and 4 h.

2.5. Vector construction and tobacco transformation

To construct the *CsSAMS1* overexpression vector, the 1182 bp full-length coding DNA sequence was amplified with primers *CsSAMS1*OE-F and *CsSAMS1*OE-R (Supplemental Table 2) using cucumber cDNA as the template. The sequenced PCR product was fused behind the CMV 35S promoter in the plant transformation vector pFGC1008-HA. The resulting *CsSAMS1*OE-HA plasmid was transformed into *Agrobacterium tumefaciens* strain EHA105. The transformation of tobacco was performed using the leaf disc-cultivation method described previously (Wang et al., 2017). Transgenic plants overexpressing *CsSAMS1* were identified by genomic PCR, qRT-PCR using specific primers (Supplemental Table 2) and western blotting using an anti-HA (Abmart, 26D11) monoclonal antibody.

2.6. Protein extraction and western blotting

For protein extraction, samples (0.5 g fresh weight) were ground in a mortar on the ice and homogenized in extraction buffer (30 mM Tris-HCl, pH 8.7, 1 mM $MgCl_2$, 0.7 M sucrose, 1 mM EDTA, 1 mM DTT, 1 mM PMSF, and 1 mM ascorbic acid). The extracted protein was quantified by the method (Bradford, 1976), denatured at 95 °C for 5 min and then stored at −20 °C until analysis. For western blotting analysis, the denatured protein (10 μg) separated by 12% sodium dodecyl sulfate-polyacrylamide gel electrophoresis (SDS-PAGE) (Laemmli, 1970) were transferred to a 0.45 μm PVDF membrane at 10 V for 1 h. The membrane was blocked for 2 h in TBST buffer (50 mM Tris, 150 mM NaCl, 0.05% Tween-20, PH 7.6) with 5% skim milk powder at room temperature, and then incubated for 1 h in TBST buffer with an anti-HA (Abmart, 26D11) monoclonal antibody. After incubation with a goat anti-mouse IgG (DyLight 800 conjugate) antibody, the membranes were detected on the LI-COR Odyssey System (LI-COR).

2.7. Salt treatment and germination detection

For germination rate detection, the wild type and transgenic lines of T_2 generation seeds were surface-sterilized and then sown on MS medium without or with 200 mM NaCl. For salt treatment, the wild type and T_2 progeny overexpression seedlings of 4–6 leaf-old were watered with or without 200 mM NaCl for 3 d. Samples were collected after being washed with distilled water for measurement of electrolyte leakage, MDA, H_2O_2, antioxidant enzyme activities, and PAs.

2.8. Measurement of electrolyte leakage, MDA and H_2O_2

Electrolyte leakage (EL) was detected according to Dhindsa et al. (1981), with some modifications. Briefly, fresh leaf sample was incubated in a 50 mL tube containing 20 mL of ddH_2O, a tube contained only 20 mL of ddH_2O was used as the control. The tubes were shaken at 100 rpm for 4 h at room temperature. The initial conductivity of the control (Cc_0) and the samples (Cs_0) was measured. Then the samples were boiled for 10 min and cooled down to the room temperature. The final conductivity (Cs_1 and Cc_1) of the control and the samples was measured as described above. EL was calculated using the formula: C (%) = $[(Cs_0–Cc_0)/(Cs_1–Cc_1)] \times 100$.

Leaf sample was homogenized in 1.6 mL of 0.1% (w/v) trichloroacetic acid (TCA) on ice and centrifuged at 12000 rpm for 20 min at 4 °C. The supernatant was collected for analysis of MDA content and H_2O_2 level. MDA measurement was detected according to Kramer et al. (1991), with slight modifications. A reaction mixture of equal volumes (1 mL) of crude extract and thiobarbituric acid (TBA) reagent (0.67% (w/v) of TBA in 10% TCA (w/v)) was heated to 99 °C for 15 min, then cooled immediately in an ice bath and centrifuged at 3000 g for 10 min. The absorbance of the supernatant was read at 532 nm and 600 nm. Data were expressed as nmol per g FW. H_2O_2 was detected according to Alexieva et al. (2010). A reaction mixture containing 0.5 mL of crude extract, 1 mL of 1 M KI, and 0.5 mL of 100 mM potassium phosphate buffer (pH 7.8) was kept in the dark for 1 h. The absorbance was measured at 390 nm, and the H_2O_2 content was calculated according to a standard curve prepared with known H_2O_2 concentrations. Data were expressed as μmol per g FW.

2.9. Detection of antioxidant enzyme activities

Leaf sample was homogenized in 1.6 mL of 50 mM cold sodium phosphate buffer (pH 7.8) on ice and centrifuged at 12000 rpm for 20 min at 4 °C. The collected supernatant was used as crude extracts to detect antioxidant enzymes activities.

SOD was analyzed by monitoring inhibition of the photochemical reduction of nitroblue tetrazolium (NBT) at 560 nm according to Gómez-Gómez and Carrasco (1996), with some modifications. The reaction mixture contained 50 mM sodium phosphate buffer (pH 7.8), 0.1 μM EDTA, 13 mM methionine, 2 μM riboflavin, 75 μM nitroblue tetrazolium chloride (NBT), and 40 μL of crude extract. Tubes were illuminated for 20 min, and the absorbance was read at 560 nm. One unit of SOD activity was defined as the amount of enzyme required to cause 50% inhibition of NBT photoreduction. Data were expressed as U per g FW.

POD and CAT were detected according to Maehly and Chance (1955), with slight modifications. The POD reaction mixture contained 50 mM sodium phosphate buffer (pH 7.0), 0.25% (v/v) guaiacol, 0.75% (v/v) H_2O_2 and 40 μL of crude extract. Changes in absorbance of the reaction solution at 470 nm were determined every 40 s. Data were expressed as U per g min. The CAT reaction mixture contained 150 mM sodium phosphate buffer (pH 7.0), 0.15% (v/v) H_2O_2 and 100 μL of crude extract. Changes in absorbance of the reaction solution at 240 nm were determined every 1 min. Data were expressed as U per g min.

APX was measured according to Nakano and Asada (1981), with some modifications. The APX reaction mixture contained 50 mM sodium phosphate buffer (pH 7.0), 85 μM EDTA-Na_2, 25 mM ascorbate, 1 mM H_2O_2, and 100 μL of crude extract. The reaction was initiated by addition of H_2O_2, and changes in absorbance of the reaction solution at 290 nm were determined every 1 min. Data were expressed as μmol ASA per g FW per h.

2.10. Measurement of PAs contents

Polyamines were extracted according to the method described by Wu et al. (2018), with slight midifications. Firstly, 0.5 g leaf sample was homogenized in 1.6 mL of 5% (w/v) cold perchloric acid (PCA) and incubated on ice for 1 h. After centrifugation at 12000 rpm and 4 °C for 20 min, the collected supernatant was used to determine the free and conjugated polyamines, and the pellet was used to determine the bound polyamines. For the free polyamines, 700 μL of the supernatant was mixed with 1.4 mL of 2 M NaOH and 15 μL of benzoyl chloride. After vortex for 30 s, the reaction mixtrue was then incubated at 37 °C for 30 min. Two milliliters of the saturated NaCl solution was added to terminate the reaction. Then 2 mL of cold diethyl ether was added to extract benzoyl polyamines. After centrifugation at 3000*g* and 4 °C for 5 min, 1 mL of the ether phase was evaporated to dryness and redissolved in 1 mL of 64% (v/v) methanol. A UPLC system (Thermo, UltiMate 3000) with a ACQUITY UPLC HSS T3 column (100 mm × 2.1 mm × 1.8 μm) and a two solvent system including a acetonitrile gradient (44–56%, v/v) at a flow rate of 0.45 mL min^{-1} was used for detecting the polyanimes. For the conjugeted polyamines, 700 μL of the supernatant was mixed with 5 mL of 6 N HCl and hydrolyzed at 110 °C for 18 h in flame-sealed glass ampoules. Then the hydrolysate was evaporated at 75 °C, and the residue was suspended in 2 ml of 5% PCA. The following steps were the same as the free polyamines extraction. For bound polyamines, the pellet was washed four times with 5% PCA and centrifuged for 5 min at 3000 g and 4 °C. Then the pellet was suspended in 5 mL of 6 N HCl then acid hydrolyzed as described above, following by the steps in accordance with the conjugeted polyamines extraction. Total polyamine content was expressed as the sum of the three forms of each polyamine.

2.11. Analysis of ACC content

The detection of ACC content was conducted by Convinced-Test company (Nanjin, China). The fresh leaf sample (0.25 g powder in in liquid nitrogen) was transferred to 50 mL tube, 5 mL deionized H_2O was added, followed by an ultrasonic water bath for 30 min. After centrifugation at 10000 rpm for 5 min at 4 °C, the supernatant was collected and adjusted the pH to 4.0. Next, 20 mL of chloroform was added and mixed vigorously, followed by the centrifugation at 10000 rpm for 5 min at 4 °C. At last, the collected supernatant was passed through the MCX column, and the eluent was used to measure ACC content by HPLC-MS/MS.

2.12. Statistical analysis

All data were analyzed using the SPSS statistics software (IBM SPSS statistics 17.0) with the independent sample *t*-test. Significance was assigned at the $P < 0.05$ level. Three or four replicates were performed per test.

3. Results

3.1. Two SAMS members were identified from the cucumber genome database

To identify *SAMS* genes in cucumber, we used the aa sequence of AtSAMSs as a probe to perform BLASTp searches in Cucumber Genome Database. After surveying the database and removing the scaffold (Csa025341) and the same (Csa001902 and Csa025763) sequences, two putative SAMS sequences were identified. We used the *CsSAMS1* (Csa001882) and *CsSAMS2* (Csa011884) designations. The full-length CDS of *CsSAMS1* and *CsSAMS2* was 1182 bp (Csa001882) and 1173 bp (Csa011884), encoding polypeptides of 393 aa, and 390 aa, respectively. The putative molecular weight was 43.2 KDa (Csa001882) and 42.6 KDa (Csa011884), with theoretical isoelectric points (PI) of 5.60 (Csa001882) and 6.51 (Csa011884). The *CsSAMS1* and *CsSAMS2* were located on chromosome 7 and chromosome 6, respectively. Both of them contained only one exon and none intron.

Multiple alignments of the predicted aa residues of CsSAMS proteins showed that CsSAMS proteins displayed a great similarity from each other (Fig. 1). The sequence of CsSAMS1 showed 90% identity and 95% similarity to that of CsSAMS2, indicating that the amino acid sequences of CsSAMS proteins exhibited a high degree of conservation. Based on the phylogenetic analysis, we found that the CsSAMS1 and CsSAMS2 protein shared high identity with their homologous of *Arabidopsis* and *Nicotiana tabacum*, compared with SAMS members from other plants (Fig. 2).

In addition, a total of 26 and 14 putative *cis-* elements related to hormone and abiotic stress response were identified in the promoter regions of the *CsSAMS1* and *CsSAMS2*, respectively (Supplemental Table 3). TGA element (involving in auxin response) and LTR element (involving low temperature response) were found in the promoter sequences of *CsSAMS1* and *CsSAMS2*. Five ABRE elements (involving in ABA response) and three CGTCA and TGAGG motifs existed in the promoter sequence of *CsSAMS1*. Moreover, there were two TCA elements (involving in salicylic acid response) and one TATC box in the promoter sequence of *CsSAMS1*. Meanwhile, multiple *cis*-elements associated with the light response, such as ATCT-motif, GATA-motif, were found in the promoter regions of *CsSAMS1* and *CsSAMS2*. In addition, one MBS element involved in drought induction was detected in *CsSAMS2*.

3.2. CsSAMS1 and CsSAMS2 displayed different expression in various organs

To investigate expression patterns of the *CsSAMS* genes in different organs, transcript levels of the *CsSAMS1* and *CsSAMS2* in the root, stem, leaf, female flower, male flower, and young fruit were analyzed. As shown in Fig. 3 A, the mRNA abundance of *CsSAMS1* in stem, male flower, and young fruit were 3.5-, 2.5- and 1.5-fold of that in root and female flower, respectively. The transcription level of *CsSAMS2* in stem and female flower was 25- and 52-fold of that in root, leaf, and young fruit respectively (Fig. 3 B). To know the mRNA abundance of these two genes in various organs, we compared their relative expression levels in every organ. As shown in Fig. 3 C, in every organ, the mRNA abundance of *CsSAMS1* was far more than that of *CsSAMS2*, which implicated that the *CsSAMS1* played a dominant role in cucumber plants.

3.3. CsSAMS1 and CsSAMS2 were involved in response to multiple hormones and abiotic stresses

The SAMS family is known to be involved in various biotic and abiotic stresses. In this study, the qRT-PCR test showed *CsSAMS1* and *CsSAMS2* were both positively responded to various hormones and abiotic stresses. Under NaCl stress, *CsSAMS1* expression in the roots maintained a rather stable level, compared with that in the leaves, which maintained steady up to 12 h but markedly decreased at 24 h (Fig. 4 A). However, the *CsSAMS2* expression in the roots was mildly induced at 2 h and remarkably up-regulated at 12 h and 24 h by NaCl stress (Fig. 4 B). The transcript levels of *CsSAMS2* in the leaves was also distinct from that of *CsSAMS1*, only an obvious peak at 6 h, but slight induced in other time points (Fig. 4 B). Similarly, in the root and leaf of cucumber seedlings, the expression level of *CsSAMS1* was higher than that of *CsSAMS2* (Fig. 4 C), suggesting that *CsSAMS1* was the main member in response to salt stress.

The transcript level of *CsSAMS1* in cucumber roots and leaves was up-regulated to about 5 folds of its basal level at 12 h after ABA application (Fig. 5 A and F). SA treatment slightly affected the expression of *CsSAMS1* in roots, while that in leaves was progressively induced to a maximum value (nearly 7 folds of its basal level) at 12 h (Fig. 5 B and G). Under MeJA treatment, the expression level of *CsSAMS1* in roots was significantly increased at 1 h but obviously decreased until 12 h (Fig. 5 C). While its mRNA level in leaves was increased to almost 9 and 12 folds of the basal level at 2 h and 12 h, respectively (Fig. 5 H). *CsSAMS1* was suppressed in roots, but up-regulated in leaves by 20% PEG during the whole process (Fig. 5 D and I). When exposed to cold, the expression level of *CsSAMS1* in roots was inhibited within 2 h, then gradually increased (Fig. 5 E). In contrary, its mRNA abundance in leaves was significantly induced at 1 h, then rapidly declined to the basal level at 2 h (Fig. 5 I).

For the *CsSAMS2*, ABA dramatically suppressed its transcription in roots during the whole experiment, while led to a 2.5, 3.9, and 2.8-fold upregulation in leaves at 2 h, 6 h, and 12 h, respectively (Fig. 6 A and F). The expression levels in roots were down-regulated by SA to varying degrees, except a stable level at 6 h (Fig. 6 B). However, its mRNA level in leaves was continuously increased to the peak value (nearly 7 folds of its basal level) at 12 h (Fig. 6 G). MeJA treatment led to higher expression in roots at 1 h and 2 h, and 12 h, but significant reductions at 6 h and 24 h (Fig. 6 C). And the transcript levels in leaves were highly induced by MeJA at 2 h, followed by a decline, which was significantly lower than its basalt level at 24 h (Fig. 6 H). Exposure to 20% PEG resulted in quick suppression at 1 h and then a 1.2–2.0-fold increase, followed by a conspicuous decrease at the end of the treatment (Fig. 6 D and I). Similarly, upon treatment with cold, the expression level in roots was sharply down-regulated at 1 h, then significantly elevated at 2 h, rapidly declined at 6 h, and quickly increased at 12 h, finally strongly suppressed at 24 h (Fig. 6 E). In leaves, apart from a significantly low transcript level at 2 h, the expression levels were 1.1–2.0-fold of its basal value within 24 h (Fig. 6 J).

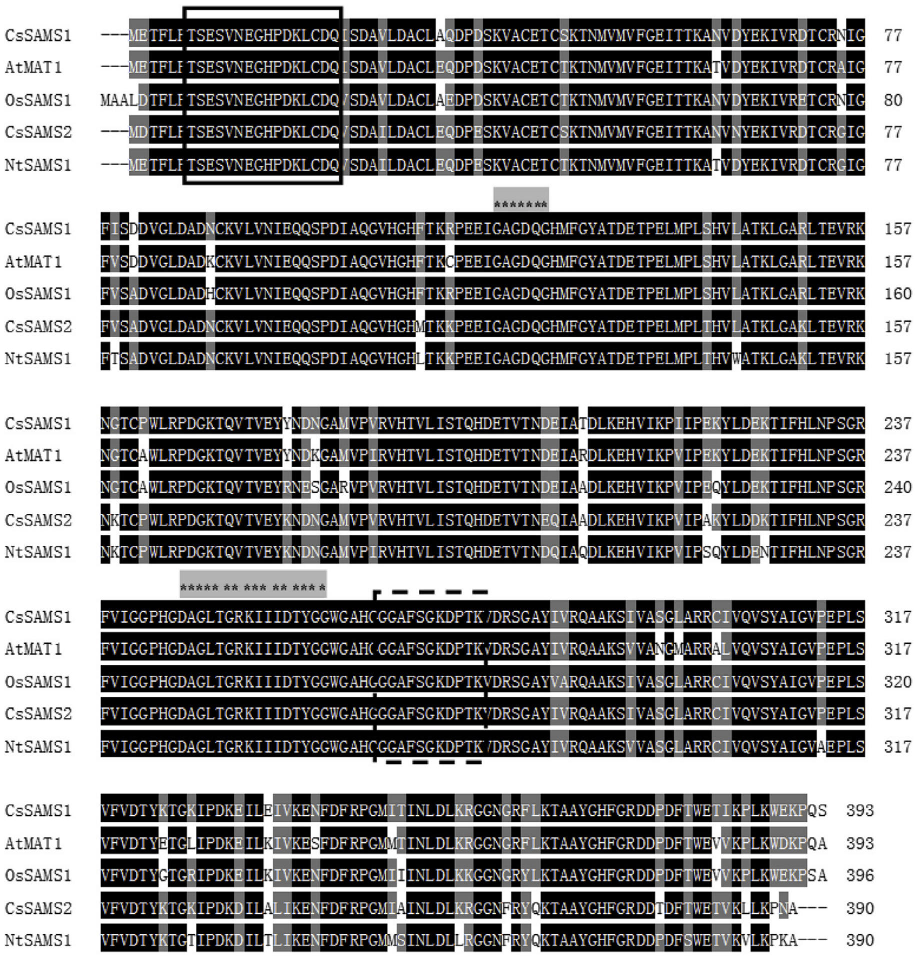

Fig. 1. Alignment of the amino acid sequences of cucumber SAMS proteins. The numbers at the end of the right side in each line are the cumulative total number of amino acids sequence in each line. Identical and similar residues were shaded in the black and gray background, respectively. The conserved domains for the ATP-binding domain were indicated by asterisks with a gray background. The putative K^+ and Mg^{2+} binding pockets were shown in a solid and dash line box, respectively.

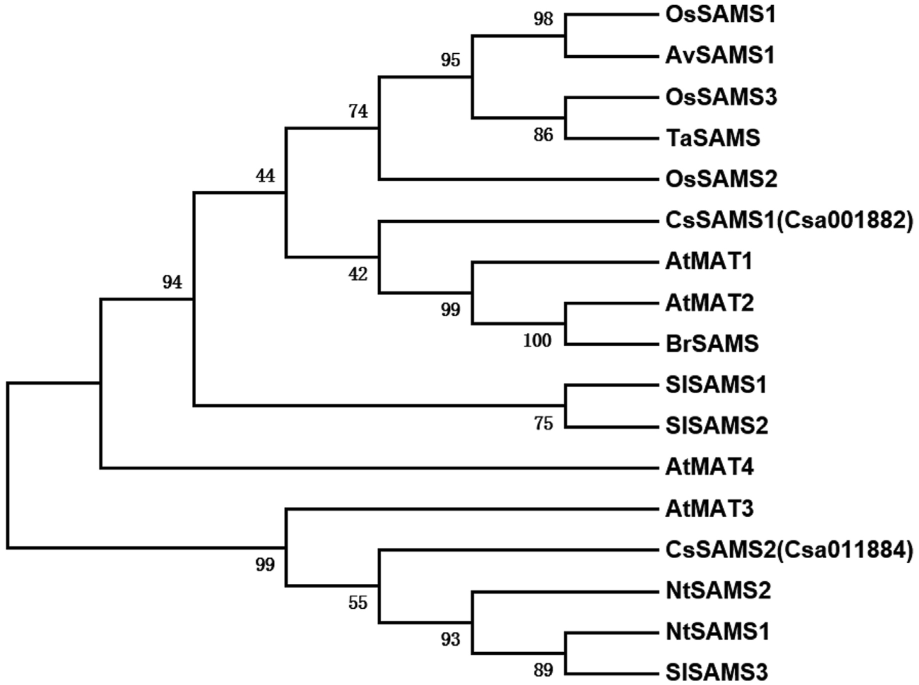

Fig. 2. Neighbor-joining phylogenetic tree of SAMS proteins of cucumber (CsSAMS1 and CsSAMS2), *Arabidopsis thaliana* (AtMAT1-AtMAT4), *Brassica rapa* (BrSAMS), *Oryza sativa* (OsSAMS1-OsSAMS3), *Triticum aestivum* (TaSAMS), *Solanum lycopersicum* (SlSAMS1-SlSAMS3), *Andropogon virginicus* (AvSAMS1) and *Nicotiana tabacum* (NtSAMS1 and NtSAMS2). The phylogenetic tree was constructed using MEGA (version 6.0) with bootstrap analysis (1000 replicates).

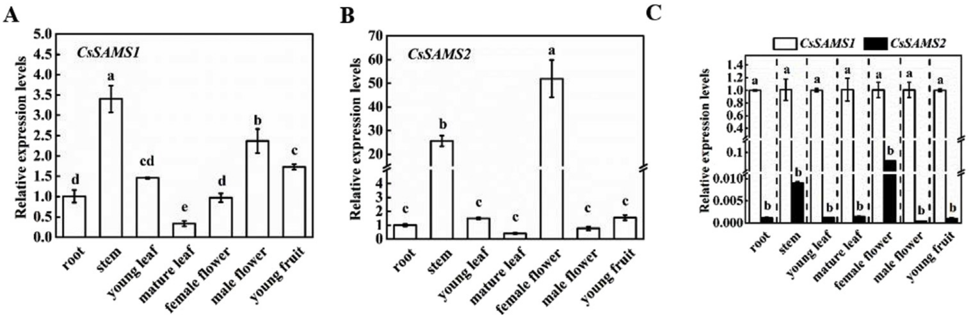

Fig. 3. Expression patterns of *CsSAMS1* and *CsSAMS2* in various organs. Total RNA was isolated from different organs of the cucumber plants. A, Expression pattern of *CsSAMS1*. B, Expression pattern of *CsSAMS2*. Expression of cucumber roots was taken as 1. C, The relative difference between *CsSAMS1* and *CsSAMS2* in different organs. Data are the mean and standard deviations of three replicates (n = 3). Different letters above the column indicate that the expression levels of *CsSAMSs* are significantly different at $P < 0.05$.

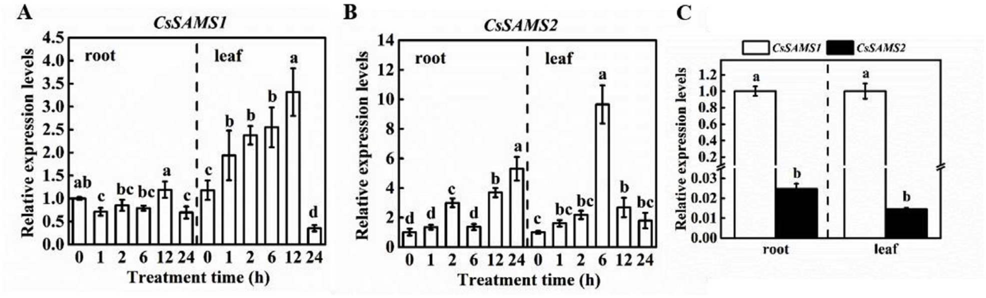

Fig. 4. Quantitative real-time PCR analysis of *CsSAMS1* and *CsSAMS2* transcripts in cucumber roots and leaves by NaCl (75 mM). The cucumber seedlings at the three-leaf stage were exposed to 75 mM NaCl in a hydroponic system. Total RNA was isolated from root or leaf samples of the cucumber seedlings at the indicated time points. A, Expression pattern of *CsSAMS1* under salt stress. B, Expression pattern of *CsSAMS2* under salt stress. Expression of 0 h treated cucumber roots or leaves was taken as 1. C, The relative difference between *CsSAMS1* and *CsSAMS2* in roots and leaves at 0 h. Data are the mean and standard deviations of three replicates (n = 3). Different letters above the column indicate that the expression levels of *CsSAMSs* are significantly different at $P < 0.05$.

3.4. Expression of CsSAMS1 enhanced salt tolerance in E.coli BL21

To examine whether CsSAMS1 could improve salt tolerance. The engineered strain overexpressing CsSAMS1 protein was constructed and its salt tolerance was investigated. A specific protein in BL21 (DE3)/pET-32a-CsSAMS1 rather than BL21 (DE3)/pET-32a (+) strain was induced by 0.1 mM IPTG after several hours (Fig. 7). The growth of BL21 (DE3)/pET-32a-CsSAMS1 strain was less sensitive to salt than BL21 (DE3)/pET-32a (+) strain in LB medium with 200, 400, and 600 mM NaCl (Fig. 8). These data suggested that expressed CsSAMS1 could enhance salt stress tolerance in *E.coli*.

3.5. Seed germination was promoted in the CsSAMS1-overexpressed lines

To further investigate the function of *CsSAMS1* in plants, three overexpression lines (OE4, OE5, OE6) were obtained and confirmed by genomic PCR and western blotting (Fig. 9 A and B). The transcript level of *CsSAMS1* of OE4, OE5, and OE6 was 15, 4, 10 folds of the level in WT, respectively (Fig. 9 C). Seed germination was significantly promoted in the overexpressing *CsSAMS1* lines, especially at the early stage (Fig. 10 A). At the third day, the germination rates of OE4, OE5, and OE6 were 50%, 38%, and 72%, respectively, whereas the WT had a germination rate of 26% (Fig. 10 B). In the presence of 200 mM NaCl, the seed germination of WT and transgenic lines were obviously inhibited. However, the transgenic lines except OE4 exhibited significant higher germination rates relative to the WT at each time point. At the end of the experiment, the germination rates of OE5 and OE6 were 58% and 38%, respectively, whereas the WT held a germination rate of 20% (Fig. 10 C). Therefore, transgenic lines OE5 and OE6 were selected for further analysis.

3.6. Overexpression of CsSAMS1 affected electrolyte leakage, MDA and H_2O_2

In order to figure out the mechanism of *CsSAMS1* in response to salt stress, the WT and transgenic seedlings were treated with 200 mM NaCl for 3 d, and their electrolyte leakage, MDA content, and H_2O_2 level were determined. Under salt stress, the leaves of transgenic lines became yellow, whereas those of WT displayed a dark green (Fig. 11 A). Under normal condition, no obvious difference in electrolyte leakage was observed among the transgenic lines and WT, while the transgenic lines exhibited significantly higher MDA level and H_2O_2 content, compared to WT (Fig. 11 B, C, and D). Under salt stress, the electrolyte leakage of OE5 was markedly lower than that of WT and OE6; the MDA contents in transgenic lines were lower than that of WT; the H_2O_2 contents of transgenic lines remained higher than that of WT (Fig. 11 B, C, and D). These findings suggested that overexpressed *CsSAMS1* in tobacco resulted in the overproduction of H_2O_2, which triggered membrane lipid peroxidation under normal growth condition, and did not contribute to improving plant salt tolerance.

3.7. Antioxidant enzyme activities were increased by overexpression of CsSAMS1

Efforts were made to investigate how the antioxidant enzyme system perform among transgenic lines and WT under normal and salt stress. Under normal condition, SOD, POD, and CAT activities of OE6, as well as POD of OE5 were significantly higher than those of WT (Fig. 12). Salt stress increased all antioxidant enzyme activities of transgenic lines and WT to varying degrees, except POD of OE6 with 40% decline compared with its control level (Fig. 12 B). In addition, it was noticeable that a significant difference was observed in POD between OE5 and OE6 under salt stress. These data implicated that overexpressed *CsSAMS1* in tobacco mainly led to the overaccumulation of H_2O_2, rather than other ROS, because its acceptor POD was extremely higher than WT under both normal condition and salt stress.

3.8. PAs and ACC content in trangenic lines changed in a CsSAMS1-expressed dependent way

In this study, PAs contents in transgenic lines and WT were detected to verify whether the overproduction of H_2O_2 ascribes to the PAs pathway. Under normal condition, OE5 displayed higher total Put and Spd contents than WT and OE6, while no significant difference was observed in total Spm content among transgenic lines and WT (Fig. 13 A, B and C). Under salt stress, however, the total Put and Spd contents

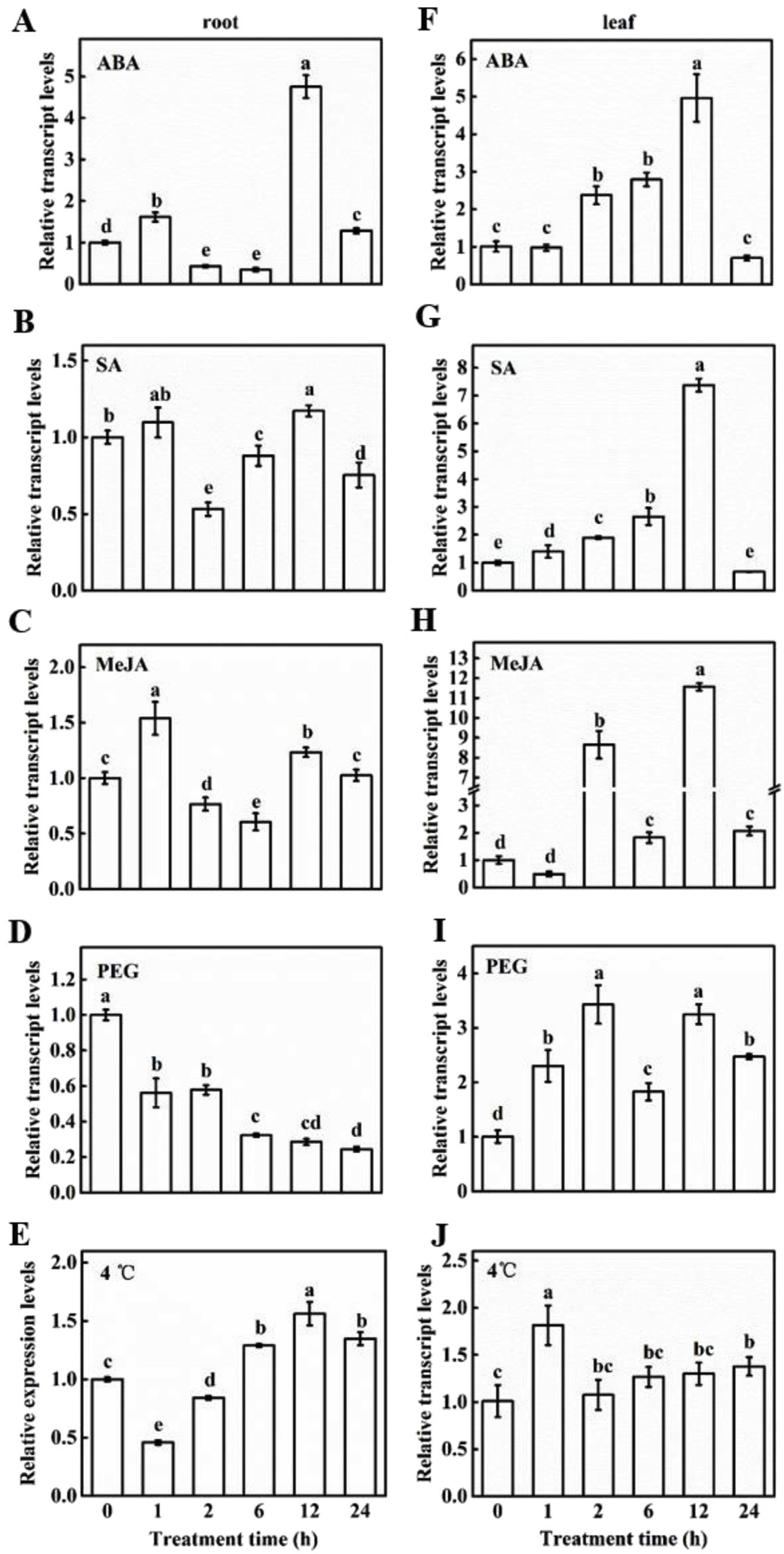

Fig. 5. Quantitative real-time PCR analysis of *CsSAMS1* expression in cucumber roots and leaves treated with 100 μM ABA (A, F), 100 μM SA (B, G), 100 μM MeJA (C, H), and 20% PEG (D, I) and 4 °C (E, J). The cucumber seedlings at the three-leaf stage were exposed to 20% PEG 6000 and 4 °C as drought and cold stress treatment, respectively, with 100 μM ABA, SA and MeJA spraying leaves, respectively, as hormones treatments. Total RNA was isolated from root and leaf samples of the cucumber seedlings at the indicated time points. Expression of 0 h treated cucumber roots or leaves was taken as 1. Data are the mean and standard deviations of three replicates (n = 3). Different letters above the column indicate that the expression levels of *CsSAMS1* are significantly different at $P < 0.05$.

of OE5 were lower than their control values, although they remained higher than WT and OE6 (Fig. 13 A and B). And all the total Spm especially that of OE5 was increased by salt stress (Fig. 13 C). Meanwhile, ACC content, the precursor of ethylene was analyzed in transgenic lines and WT. As shown in Fig. 13 D, obviously less ACC content was detected in OE6 under both normal condition and salt stress. And compared with WT, the OE5 had less ACC under normal condition, but more ACC under salt stress. All these results above

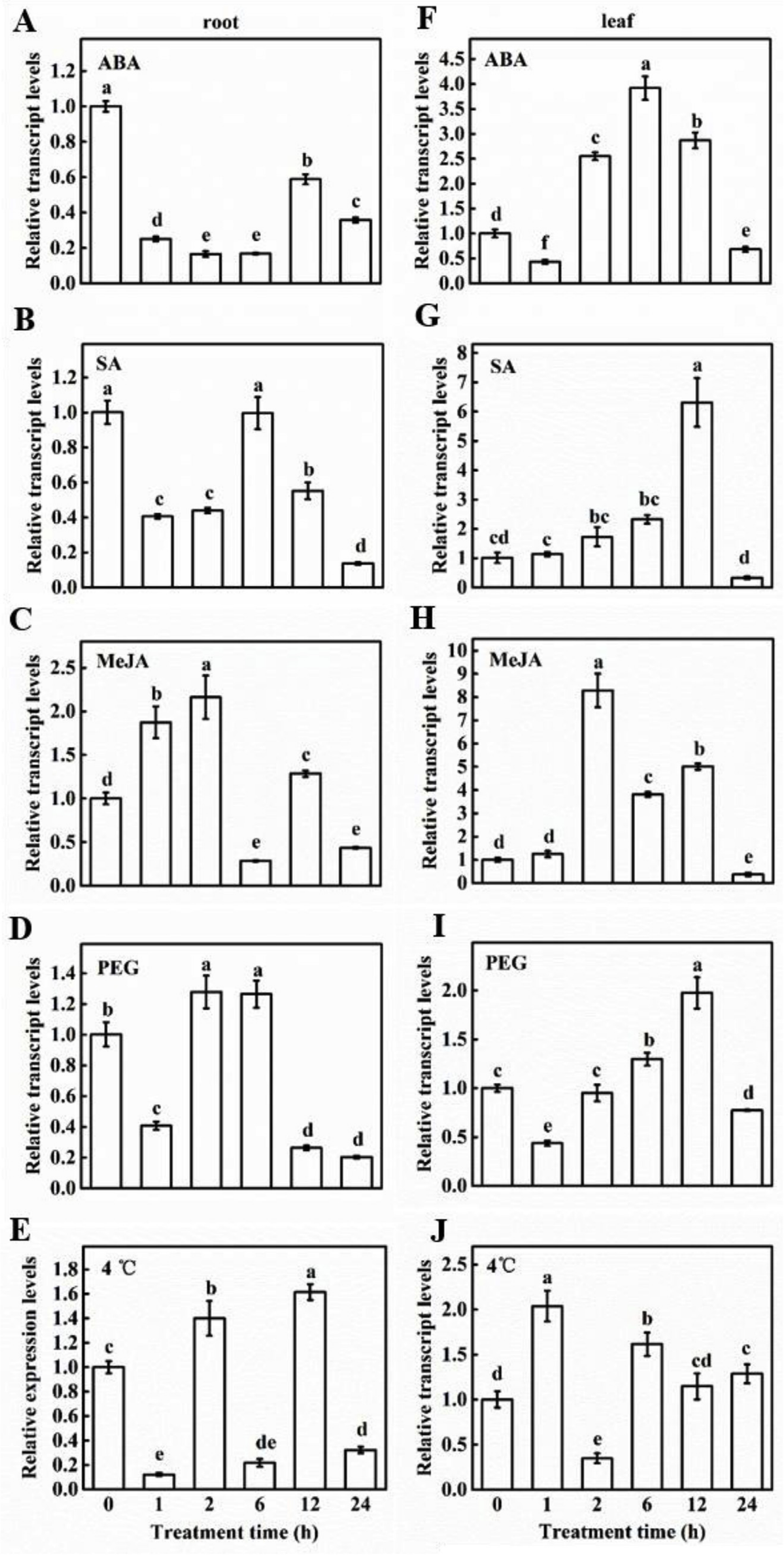

Fig. 6. Quantitative real-time PCR analysis of *CsSAMS2* expression in cucumber roots and leaves treated with 100 μM ABA (A, F), 100 μM SA (B, G), 100 μM MeJA (C, H), and 20% PEG (D, I) and 4 °C (E, J). The cucumber seedlings at the three-leaf stage were exposed to 20% PEG 6000 and 4 °C as drought and cold stress treatment, respectively, with 100 μM ABA, SA and MeJA spraying leaves, respectively, as hormones treatments. Total RNA was isolated from root and leaf samples of the cucumber seedlings at the indicated time points. Expression of 0 h treated cucumber roots or leaves was taken as 1. Data are the mean and standard deviations of three replicates (n = 3). Different letters above the column indicate that the expression levels of *CsSAMS2* are significantly different at $P < 0.05$.

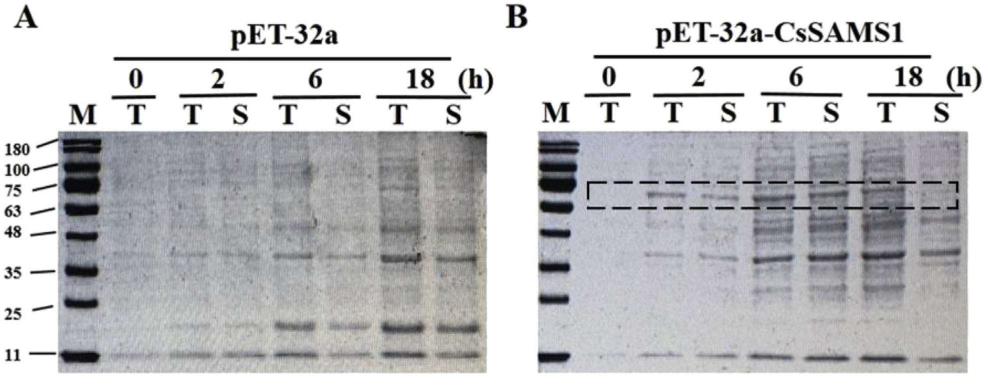

Fig. 7. CsSAMS1 proteins expressed in *E.coli* and separated by SDS-PAGE. A, BL21 (DE3)/pET-32a. B, BL21 (DE3)/pET-32a-CsSAMS1. M, Molecular-mass markers (kDa); T, Total protein; S, Soluble protein. The expressed CsSAMS1 proteins were indicated by a dash box.

indicated that the overproduction of H_2O_2 in OE5 was probably caused by enhancing PAs levels, while low PAs in OE6 might ascribe to the overproduction of ethylene.

3.9. Overexpression of CsSAMS1 influenced the transcription of genes relative to the antioxidant system, PAs metablism, and Ethylene synthesis.

Transcriptional level analysis for genes relative to PAs metabolism, antioxidant system, and ethylene systhesis was shown in Fig. 14. Under normal growth conditions, *ACO*, a key enzyme for ethylene synthesis, was significantly induced in transgenic lines, whereas the transcription level of *SAMDC*, an important enzyme introducing SAM into PAs pathway, was lower than that in wild type. Under salt stress, however, *ACO* was significantly decreased, but the expressions of *SAMDC*, *SPDS*, and *SPMS* were all up-regulated. These data suggested that the synthesis of ethylene was enhanced in transgenic lines under non-stress conditions, probably to regulate plant height, whereas overexpression of *CsSAMS1* accelerated polyamine synthesis to response to salt stress. It was noticeable that the expression levels of *SOD* and *CAT*, as well as *SPDS* in transgenic lines, were higher than those in WT. In addition, the transcription level of *PAO* was markedly higher than that of WT under salt stress.

4. Discussion

Salinity is a major abiotic stress. High salt stress inhibits crops growth by overly accumulating Na^+ to disrupt the homeostasis of water potential and ion distribution. S-adenosylmethionine synthetase (SAMS) is the unique enzyme catalyzing the synthesis of S-adenosylmethionine (SAM), which is not only an important methyl donor but also a common precursor for the synthesis of polyamines and ethylene (Roje, 2006; Grillo and Colombatto, 2008). In plants, a growing body of

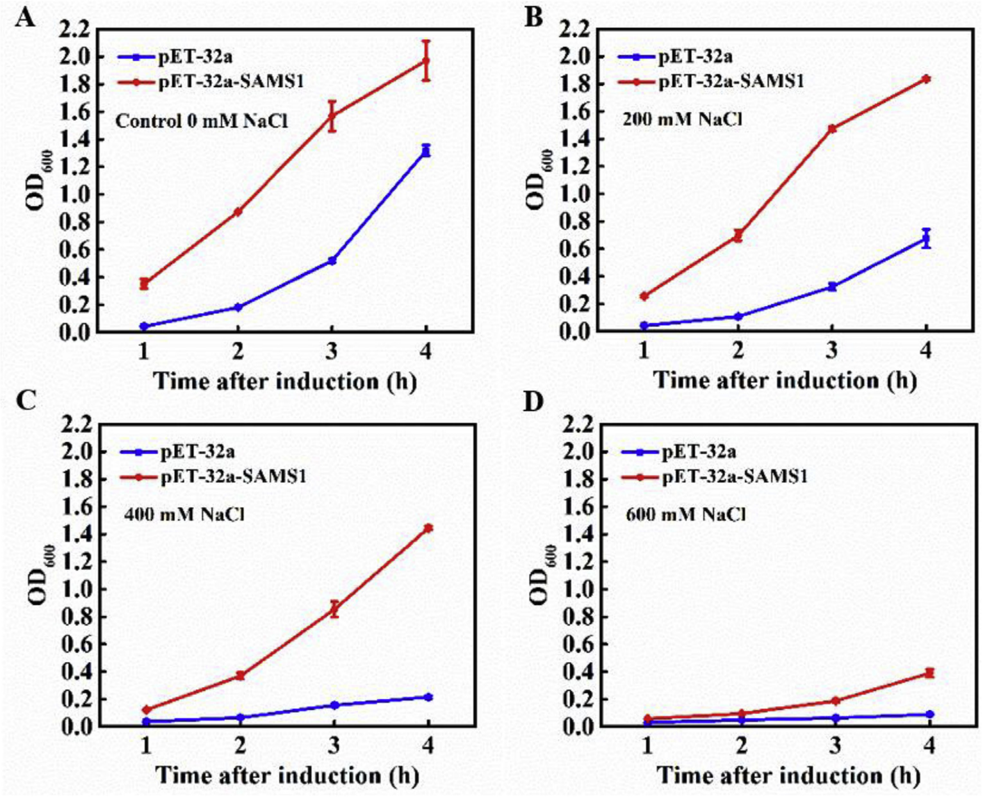

Fig. 8. Growth curves of BL21/pET-32a and BL21/pET-32a-CsSAMS1 in the presence of Na^+. Cells induced by 0.1 mM IPTG for 4 h were transferred to LB media without (A) or with 200 (B), 400 (C), 600 (D) mM NaCl. Data are the mean and standard deviations of three replicates (n = 3).

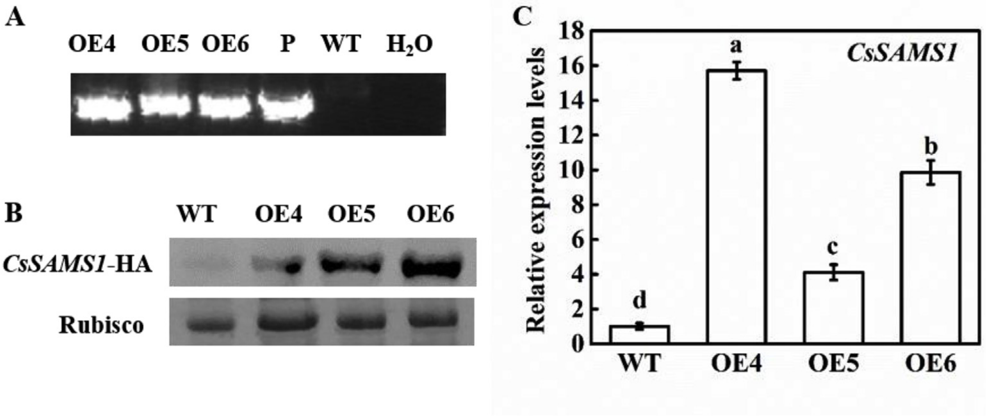

Fig. 9. Identification of the overexpression *CsSAMS1*-transgenic tobacco. A, Genomic DNA amplification in wild type and overexpression transgenic plants. P, Plasmid harboring *CsSAMS1*, as the positive control. WT, Wild type. B, CsSAMS1 protein levels in the leaves of WT and overexpression transgenic plants. C, QRT-PCR tested in transgenic lines and wild type. Total RNA was isolated from the leaves of WT and overexpression transgenic plants. Expression of WT was taken as 1. The Rubisco large subunit was used as a loading control. Data are the mean and standard deviations of three replicates (n = 3). Different letters above the column indicate that the expression levels of *CsSAMS1* genes are significantly different at $P < 0.05$.

SAMS members from various species have been proved to involve in development and stress response (Lindroth et al., 2001; Pulla et al., 2009; Quan et al., 2014; Kim et al., 2015; Ezaki et al., 2016). To date, however, the majority of reports on SAMS mainly focused on their expression profiles, and there was less about the mechanism by which regulating plant development and stress response. In the present study, we characterized two *SAMS* members in cucumber, and then analyzed their function under salt stress by introducing *CsSAMS1* into *E.coli* BL21 strain and tobacco plants.

All SAMS members discovered so far, contain an N-terminal domain with the methionine binding site, the central domain and the C-terminal domain with the ATP binding motif (Markham and Pajares, 2009), which suggests their high conservation during species evolution. Multiple sequence alignment revealed that the CsSAMS1 and CsSAMS2 shared the high identity and were close to those of *Arabidopsis* and tobacco, respectively (Fig. 1). The phylogenetic analysis was consistent with the multiple sequence alignment, showing that CsSAMS1 and CsSAMS2 were in the same group with AtMAT1 and NtSAMS2, respectively (Fig. 2). These findings implicated that the *CsSAMS1* and *CsSAMS2* may possess a redundant but somewhat different function. In addition, from gene structure analysis, we found that *CsSAMS1* and *CsSAMS2* both had only one exon and no intron, which suggested that their complete function was prone to be affected by gene structure changes. RNAi of highly conserved 281 bp in the open reading frame (ORF) of *OsSAMS1* not only repressed the transcript level of *OsSAMS1* but also inhibited the expressions of *OsSAMS2* and *OsSAMS3*, finally resulted in dwarfism, late germination and low fertility (Li et al., 2011). These results indicate that *CsSAMS* genes are conservative and may play important in plant development.

Compared with leaf and root, *CsSAMS1*and *CsSAMS2* were highly expressed in stem (Fig. 3 A and B). This expression pattern is similar to those of early maturing barley (Kim, 2013), *Medicago sativa* subsp. *falcate* (Guo et al., 2014) and potato (Kim et al., 2015), with SAMS mRNA abundance in stem much higher than that in root. In contrast, in several species, the *SAMS* predominately expressed in root rather than other tissues, such as in pea (*Pisum sativum*) (Gómez-Gómez and Carrasco, 1998), *Pinus contorta* (Lindroth et al., 2001), *Panax ginseng* (Pulla et al., 2009), and in rice (Li et al., 2011). It was noticed that the expression level of *CsSAMS1* in each organ was far higher than that of *CsSAMS2*, and interestingly, *CsSAMS1* was highly expressed in male flower, whereas the mRNA abundance of *CsSAMS2* was preferentially accumulated in female flower (Fig. 3). Similarly, in *Arabidopsis*, *AtMAT1* and *AtMAT2* (also named *AtSAMS1* and *AtSAMS2*) were expressed in almost all tissues, whereas *AtMAT3* was expressed predominantly in pollen (Mao et al., 2015; Chen et al., 2016). These results show that *CsSAMS1* and *CsSAMS2* both perform an important role in plant development, and will guide our future work to figure out whether they play a critical role in flower development.

SAMS has been considered as an important stress gene in response to a variety of abiotic stresses. In tomato, three *SAMS* members in roots, stems, and leaves, exhibited different extent of mRNA abundance changes under NaCl, mannitol, and ABA (Espartero et al., 1994). It was also reported that four *HvSAMS* genes in leaves were differentially response to NaCl and ABA, although they belonged to the same group (Kim, 2013). In this study, multiple *cis*-elements relative to hormones and stresses were found in the promoter sequences of *CsSAMS1* and *CsSAMS2* (Supplemental Table 3). The differential expression profiles of the *CsSAMS1* and *CsSAMS2* in roots and leaves were observed under stimuli, including NaCl, ABA, SA, MeJA, drought, and low temperature (Figs. 5 and 6). The expression level of *CsSAMS1* in leaves was progressively up-regulated within 12 h, and that of *CsSAMS2* changed dramatically at 6 after salt stress. Many studies have confirmed that *SAMS* is a salt-induced gene. The *SlSAMS1* gene transcript level was significantly up-regulated by NaCl treatment (Sanchez-Aguayo et al., 2004). The transcript level of *LrSAMS* was obviously induced by 400 mM NaCl from 3 h and reached a maximal level at 24 h (Li et al., 2013c). In addition, the increasing changes under salt stress were found in *Panax ginseng* (Pulla et al., 2009), wheat (Kamal et al., 2012), potato (Kim et al., 2015) and soybean (Wang et al., 2016). ABA is an important stress hormone that mediates a series of plant responses to abiotic

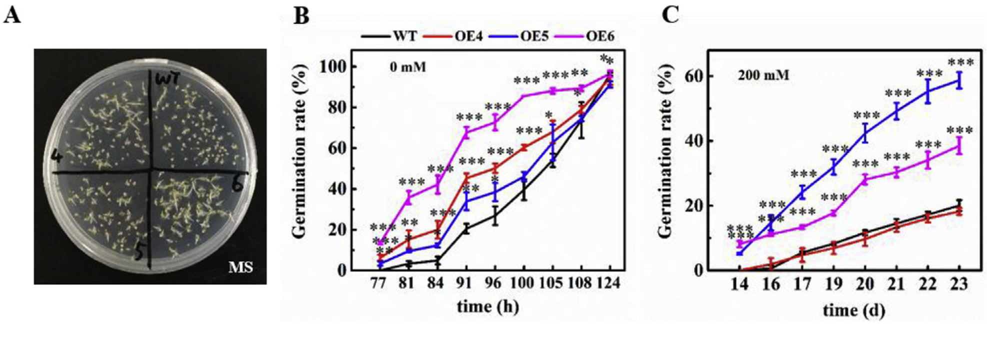

Fig. 10. Seed germination of wild type (WT) and transgenic lines (OE4, OE5 and OE6). A, Phenotype of seed germination on the MS plate. B and C, Time-course change of seed germination rate. Error bars represent standard deviations for three plates. Asterisks indicate significant difference between WT and transgenic lines at the same time point (*$P < 0.05$, **$P < 0.01$, ***$P < 0.001$).

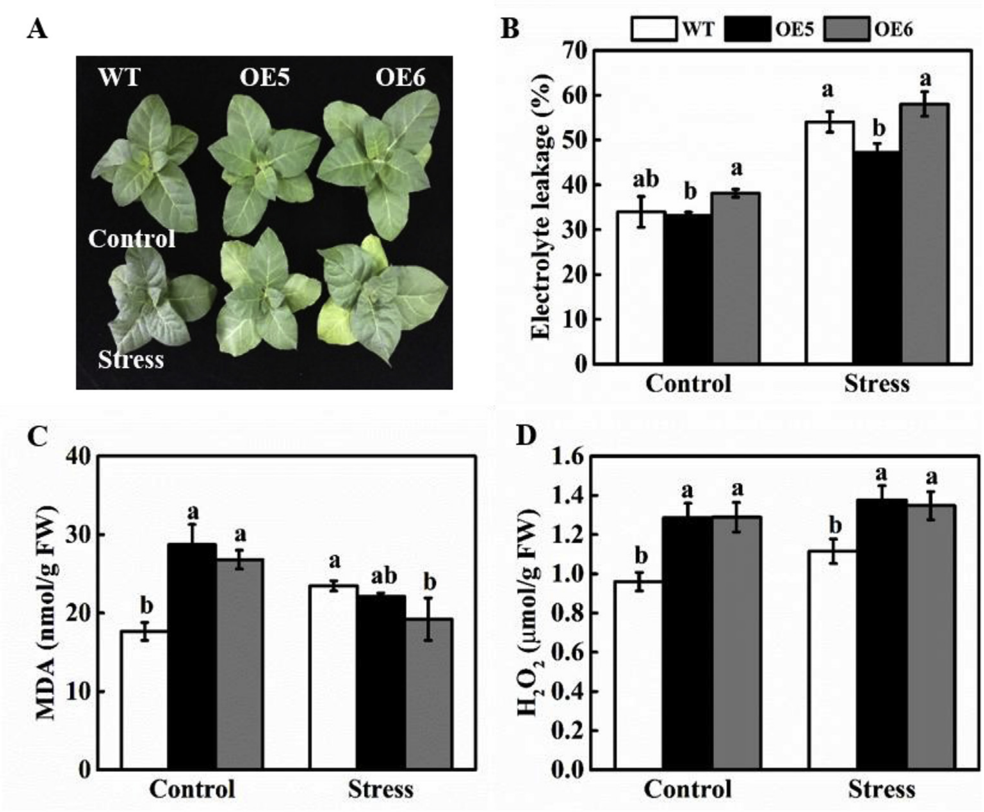

Fig. 11. Seedlings growth and electrolyte leakage, MDA, H_2O_2 detection of wild type (WT) and transgenic plants (OE5 and OE6) under salt stress treatment. A, Phenotype of tobacco seedlings. B, Electrolyte leakage. C, MDA content. D, H_2O_2 content. Error bars represent standard deviations for three replicates. Different letters represent significant differences at $P < 0.05$.

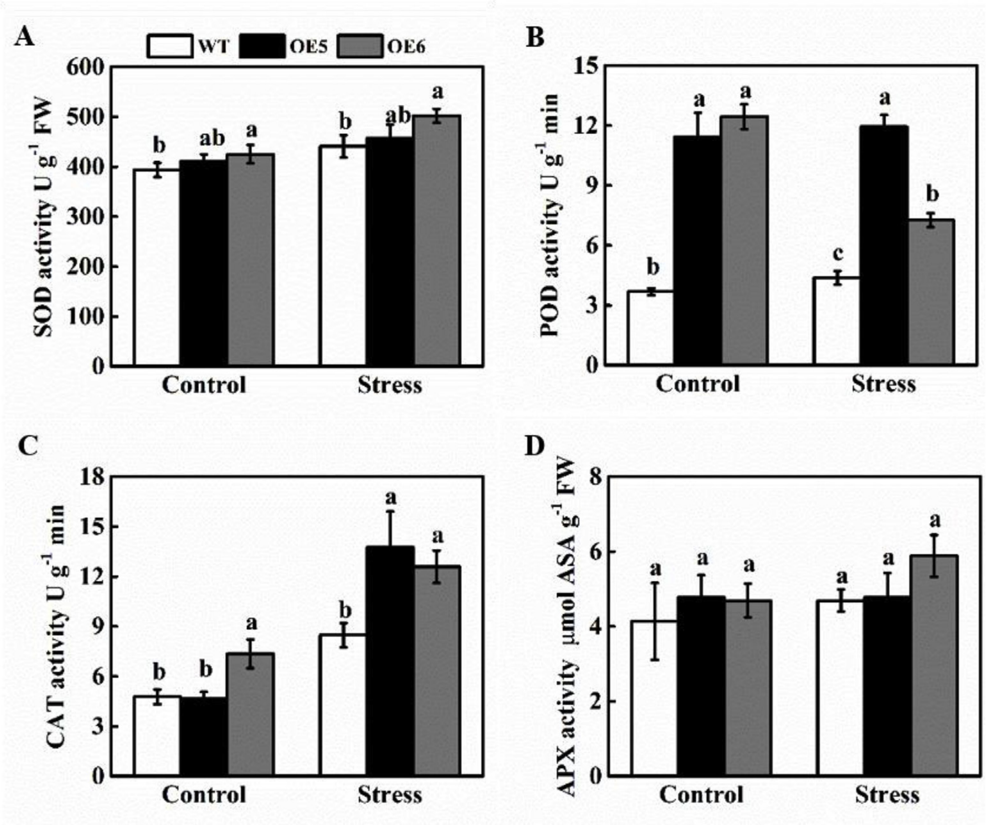

Fig. 12. Effects of salt stress on antioxidant enzyme activity in both wild type (WT) and transgenic tobacco leaves. A, SOD activity. B, POD activity. C, CAT activity. D, APX activity. Data are the mean and standard deviations of three replicates (n = 3). Different letters represent significant differences at $P < 0.05$.

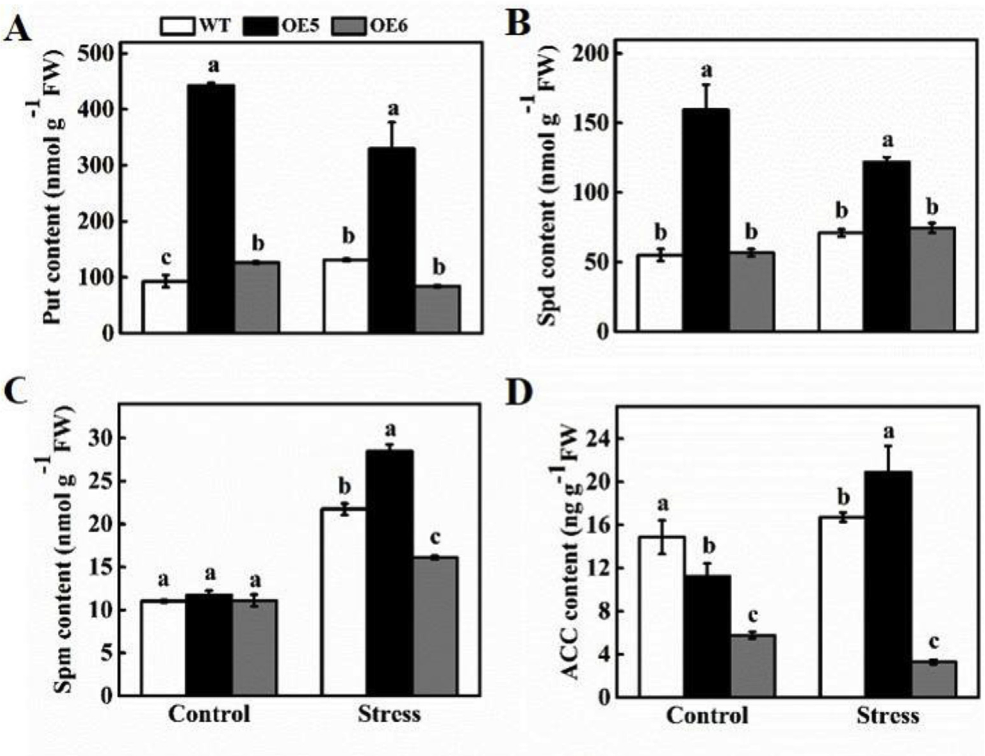

Fig. 13. Effects of salt stress on total Put content (A), total Spd content (B), total Spm content (C), and ACC content (D) in both wild type (WT) and transgenic tobacco leaves. Data are the mean and standard deviations of three replicates (n = 3). Different letters represent significant differences at $P < 0.05$.

stresses. In leaves, the expression patterns of *CsSAMS1* and *CsSAMS2* by ABA and SA were both progressively up-regulated, suggesting that they may be involved in abiotic stresses response in an ABA and SA-dependent manner. In roots, ABA markedly induced the expression of *CsSAMS1* at several time points, while inhibited the expression of *CsSAMS2* during the whole experiment. In contrast, PEG significantly decreased the expression of *CsSAMS1* in roots but induced the expression of *CsSAMS2* at 2 and 6 h. These expression patterns may be relative to the phenomena that ABRE elements involved in ABA response were present in the promoter sequence of *CsSAMS1* and the promoter sequence of *CsSAMS2* containing a drought response element. The effect of MeJA on *CsSAMS1* and *CsSAMS2* in cucumber seedlings appeared to be more interesting. The expression levels of *CsSAMS1* and *CsSAMS2* in roots was obviously up-regulated at 1 h, whereas their inductions in leaves occurred later, with peak values higher than those of other stimuli. These results indicated that MeJA may not directly regulate the function of cucumber *SAMS* but probably played an important role in their functions. In addition, *CsSAMS1* and *CsSAMS2* with LTR *cis*-element were transcriptionally activated or suppressed by cold within 24 h. Taken together, *CsSAMS1* and *CsSAMS2* both responded to hormones and abiotic stresses, suggesting that they may function independently or synergistically during plant development and stress response.

In this study, we found that expressed CsSAMS1 in *E.coli* BL21 strain could enhance their salt tolerance, which was reflected by the fast growth in the present of Na$^+$. This result was consistent with the observation of LrSAMS protein expressed in *E.coli* (Li et al., 2013c). Recently, an Av*SAMS* gene, obtained from candidate clones which conferred Al tolerance to yeast transformants, was introduced into *Arabidopsis thaliana* to confirm its benefit to improving Al stress (Ezaki et al., 2016). In this study, overexpression *CsSAMS1* lines were obtained but unfortunately we could not measure the SAMS activity *in vivo* because the SAM is low in plant tissues for its fast degradation (Mao et al., 2015). SAM in plants flows into other pathways besides participating in the synthesis of PAs and ethylene (Roje, 2006; Grillo and Colombatto, 2008). The majority of reports hold the view that the improvement of stress tolerance in overexpressing SAMS plants attributes to the accumulation of polyamines. For example, transgenic tobacco overexpressing *SsSAMS2* accumulated higher levels of free polyamines and suffered less hurt from salt stress (Qi et al., 2010). Overexpression of *MfSAMS1* enhanced polyamine synthesis and oxidation, which in turn improved antioxidant protection, resulted in low sensitivity to cold stress in transgenic plants (Guo et al., 2014). Overexpression of *SlSAMS1* increased tomato callus tolerance to alkali stress through polyamine and H_2O_2 cross-linked networks (Gong et al., 2016). Overexpression of *BvM14-SAMS2* enhanced *Arabidopsis* tolerance to salt and alleviate stress damage by accumulating Spd and Spm (Ma et al., 2017). In this study, under salt stress, OE5 displayed a higher gernimation rate than OE4 and OE6, which contained higher transcript levels of *CsSAMS1*. Significantly higher contents of MDA and H_2O_2, as well as enhanced antioxidant enzyme activities, were observed in transgenic lines under non-stress conditions. Moreover, we found that changes of PAs and ACC contents in overexpression *CsSAMS1* lines exhibited a *CsSAMS1*-expressed dependent way. PAO was considered as one of the key factors to trigger oxidative burst (Yoda et al., 2006). A series of studies confirmed that PAO-induced H_2O_2 exerted multiafaceted roles on plant growth and stress responses (Moschou et al., 2008, 2010; Moschou and Roubelakisangelakis, 2014; Gémes et al., 2017). Overexpression of *CsPAO4* promoted seed germination, whereas inhibited root elongation under salt stress (Wang and Liu, 2016). According to all results in the present study, we speculate that higher expression of *CsSAMS1* in plants may exert similar functions with PAO-induced H_2O_2, which plays a complex role in plant development and stress responses. At least, we could confirm that a proper overexpression of *CsSAMS1* is beneficial for salt tolerance. Next, more work is required to clarify whether ROS burst is induced by overexpressing Cs*SAMS1*, which does not contribute to stress tolerance, especially to the sat tolerance.

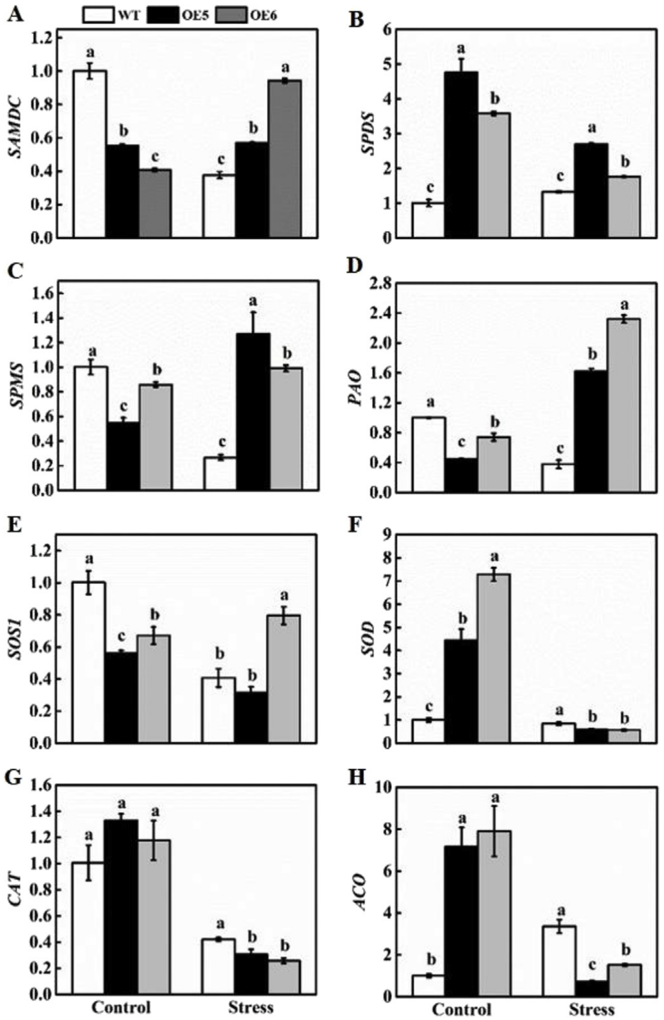

Fig. 14. Effects of salt stress on relative gene expression of NtSAMDC (A), NtSPDS (B), NtSPMS (C), NtPAO (D), NtSOS1 (E), NtSOD (F), NtCAT (G), and NtACO (H) in both wild type (WT) and transgenic tobacco leaves. Data are the mean and standard deviations of three replicates (n = 3). Different letters represent significant differences at $P < 0.05$.

5. Conclusions

Taken together, we identified two *SAMS* members in cucumber, designated as *CsSAMS1* and *CsSAMS2*. They shared high similarity to each other and highly conserved with members of other species, especially *AtSAMSs* and *NtSAMSs*. The *CsSAMS1* and *CsSAMS2* both highly expressed in stems and flowers suggests that *CsSAMS* play an important role in vascular and flower development. In addition, *CsSAMS1* and *CsSAMS2* exhibited distinct responses to hormones and abiotic stresses. Overexpressed *CsSAMS1* in tobacco plants and *Escherichia coli* BL21 (DE3) confirmed that *CsSAMS1* was a candidate gene improving plant development and salt tolerance. It will be required for future studies to provide more explorations and evidence to explain the role of *CsSAMS1* in plant growth and stress response.

Author contribution statement

SR Guo designed the research project. MW He performed the research and wrote the paper. JQ Wu collaboratively prepared RNA samples for the experiments. Y Wang modified this manuscript. S Shu and J Sun analyzed the data. All authors reviewed and approved the manuscript.

Conflicts of interest

The authors declare that they have no conflict of interests.

Accession numbers

Sequence data from this article can be found in the Cucumber Genome Database or NCBI database under the following accession numbers:CsSAMS1 (Csa001882), CsSAMS2 (Csa011884), NP_171751 (AtMAT1), NP_192094 (AtMAT2), NP_181225 (AtMAT3), NP_188365 (AtMAT4), AIR95994 (OsSAMS1), XP_015613535 (OsSAMS2), XP_015614349 (OsSAMS3), AB907169 (AvSAMS1), NP_001312332 (NtSAMS1), NP_001312727 (NtSAMS2), AAV80205 (BrSAMS), ABY85789 (TaSAMS), NP_001234425 (SlSAMS1), NP_001296305 (SlSAMS2), NP_001304005 (SlSAMS3).

Contributions

SR Guo designed the research project. MW He performed the research and wrote the manuscript. JQ Wu collaboratively prepared RNA samples for the experiments. Y Wang modified this manuscript. S Shu and J Sun analyzed the data.

Acknowledgments

This work was supported by the National Natural Science Foundation of China (No. 31471869 and No. 31672199), the China Earmarked Fund for Modern Agro-industry Technology Research System (CARS-23-B12).

Appendix

Aa	amino acid
ABA	abscisic acid
ACC	1-aminocyclopropane-1-carboxylate
ACS	ACC synthase
ACO	ACC oxidase
APX	ascorbate peroxidase
ATP	adenosine triphosphate
bp	base pair
CAT	catalase
CDS	coding DNA sequence
DO	dissolved oxygen
DTT	dithiothreitol
IPTG	isopropyl β-D-thiogalactoside
MDA	malondialdehyde
MeJA	methyl jasmonate
NBT	nitroblue tetrazolium
OE	overexpressing
ORF	open reading frame
PAs	polyamines
PAO	polyamine oxidase
Put	putrescine
PEG	polyethylene glycol
PMSF	phenylmethyl sulfanyl fluoride
POD	peroxidase
PVDF	polyvinylidene fluoride
qRT-PCR	quantitative real-time PCR
RNAi	RNA interference
ROS	Reactive oxygen species
RT-PCR	reverse transcript PCR
SA	salicylic acid
SAM or AdoMet	S-adenosylmethionine
SAMDC	S-adenosylmethionine decarboxylase
SAMS	S-adenosylmethionine synthase
Spd	spermidine

SPDS	spermidine synthases
Spm	spermine
SPMS	spermine synthase
SOD	superoxide dismutase
SOS	salt overly sensitive
WT	wild type

Appendix A. Supplementary data

Supplementary data to this article can be found online at https://doi.org/10.1016/j.plaphy.2019.06.006.

References

Alexieva, V., Sergiev, I., Mapelli, S., Karanov, E., 2010. The effect of drought and ultraviolet radiation on growth and stress markers in pea and wheat. Plant Cell Environ. 24, 1337–1344.

Boerjan, W., Bauw, G., Van, M.M., Inzé, D., 1994. Distinct phenotypes generated by overexpression and suppression of S-adenosyl-L-methionine synthetase reveal developmental patterns of gene silencing in tobacco. Plant Cell 6, 1401–1414.

Bradford, M., 1976. A rapid and sensitive method for quantitation of microgram quantities of protein utilizing the principle of proteindye binding. Anal. Biochem. 72, 248–254.

Bregoli, A.M., Scaramagli, S., Costa, G., Sabatini, E., Ziosi, V., Biondi, S., Torrigiani, P., 2002. Peach (*Prunus persica*) fruit ripening: aminoethoxyvinylglycine (AVG) and exogenous polyamines affect ethylene emission and flesh firmness. Physiol. Plantarum 114, 472–481.

Breusegem, F.V., Dekeyser, R., Gielen, J., Montagu, M.V., Caplan, A., 1994. Characterization of a S-adenosylmethionine synthetase gene in rice. Plant Physiol. 105, 1463–1464.

Burstenbinder, K., Rzewuski, G., Wirtz, M., Hell, R., Sauter, M., 2007. The role of methionine recycling for ethylene synthesis in *Arabidopsis*. Plant J. 49, 238–249.

Chen, Y., Zou, T., McCormick, S., 2016. S-adenosylmethionine synthetase 3 is important for pollen tube growth. Plant Physiol. 172, 244–253.

Dhindsa, R.S., Plumb-Dhindsa, P., Thorpe, T.A., 1981. Leaf senescence: correlated with increased levels of membrane permeability and lipid peroxidation, and decreased levels of superoxide dismutase and catalase. J. Exp. Bot. 32, 93–101.

Espartero, J., Pintor-Toro, J.A., Pardo, J.M., 1994. Differential accumulation of S -adenosylmethionine synthetase transcripts in response to salt stress. Plant Mol. Biol. 25, 217–227.

Ezaki, B., Higashi, A., Nanba, N., Nishiuchi, T., 2016. An S-adenosyl methionine synthetase (*SAMS*) gene from *Andropogon virginicus* L. confers aluminum stress tolerance and facilitates epigenetic gene regulation in *Arabidopsis thaliana*. Front. Plant Sci. 7, 1627.

Gémes, K., Mellidou, I., Karamanoli, K., Beris, D., Park, K.Y., Matsi, T., Haralampidis, K., Constantinidou, H.I., Roubelakis-Angelakis, K.A., 2017. Deregulation of apoplastic polyamine oxidase affects development and salt response of tobacco plants. J. Plant Physiol. 211, 1–12.

Gómez-Gómez, L., Carrasco, P., 1996. Hormonal regulation of S-adenosylmethionine synthase transcripts in pea ovaries. Plant Mol. Biol. 30, 821–832.

Gómez-Gómez, L., Carrasco, P., 1998. Differential expression of the S-adenosyl-L-methionine synthase genes during pea development. Plant Physiol. 117, 397–405.

Gong, B., Li, X., VandenLangenberg, K.M., Wen, D., Sun, S., Wei, M., Li, Y., Yang, F., Shi, Q., Wang, X., 2014. Overexpression of S-adenosyl-L-methionine synthetase increased tomato tolerance to alkali stress through polyamine metabolism. Plant Biotechnol. J. 12, 694–708.

Gong, B., Wang, X., Min, W., Yang, F., Yan, L., Shi, Q., 2016. Overexpression of S-adenosylmethionine synthetase 1 enhances tomato callus tolerance to alkali stress through polyamine and hydrogen peroxide cross-linked networks. Plant Cell Tissue Organ Cult. 124, 377–391.

Grillo, M.A., Colombatto, S., 2008. S-adenosylmethionine and its products. Amino Acids 34, 187–193.

Guo, Z., Tan, J., Zhuo, C., Wang, C., Xiang, B., Wang, Z., 2014. Abscisic acid, H_2O_2 and nitric oxide interactions mediated cold-induced S-adenosylmethionine synthetase in *Medicago sativa* subsp. *falcata* that confers cold tolerance through up-regulating polyamine oxidation. Plant Biotechnol. J. 12, 601–612.

Gupta, K., Dey, A., Gupta, B., 2013. Plant polyamines in abiotic stress responses. Acta Physiol. Plant. 35, 2015–2036.

Kamal, A.H., Cho, K., Kim, D.E., Uozumi, N., Chung, K.Y., Lee, S.Y., Choi, J.S., Cho, S.W., Shin, C.S., Woo, S.H., 2012. Changes in physiology and protein abundance in salt-stressed wheat chloroplasts. Mol. Biol. Rep. 39, 9059–9074.

Kim, J.Y., 2013. Identification and functional analysis of S-adenosylmethionine synthetase (*HvSAMS*) genes in early maturing barley (*Hordeum vulgare* subsp. *vulgare*). Plant Breed. Biotech. 1, 178–195.

Kim, S.B., Yu, J.G., Lee, G.H., Park, Y.D., 2012. Characterization of *Brassica rapa* S-adenosyl-L-methionine synthetase gene including its roles in biosynthesis pathway. Hort. Environ. Biotechnol. 53, 57–65.

Kim, S.H., Kim, S.H., Palaniyandi, S.A., Yang, S.H., Suh, J.W., 2015. Expression of potato S-adenosyl-L-methionine synthase (*SbSAMS*) gene altered developmental characteristics and stress responses in transgenic *Arabidopsis* plants. Plant Physiol. Biochem. 87, 84–91.

Kramer, G.F., Norman, H.A., Krizek, D.T., Mirecki, R.M., 1991. Influence of UV-B radiation on polyamines, lipid peroxidation and membrane lipids in cucumber. Phytochemistry 30, 2101–2108.

Kusano, T., Berberich, T., Tateda, C., Takahashi, Y., 2008. Polyamines: essential factors for growth and survival. Planta 228, 367–381.

Laemmli, U.K., 1970. Cleavage of structural proteins during the assembly of the head of bacteriophage T4. Nature 227, 680–685.

Li, B., He, L., Guo, S., Li, J., Yang, Y., Yan, B., Sun, J., Li, J., 2013a. Proteomics reveal cucumber Spd-responses under normal condition and salt stress. Plant Physiol. Biochem. 67, 7–14.

Li, B., Sang, T., He, L., Sun, J., Li, J., Guo, S., 2013b. Exogenous spermidine inhibits ethylene production in leaves of cucumber seedlings under NaCl Stress. J. Am. Soc. Hortic. Sci. 138, 108–113.

Li, W., Han, Y., Tao, F., Chong, K., 2011. Knockdown of *SAMS* genes encoding S-adenosyl-L-methionine synthetases causes methylation alterations of DNAs and histones and leads to late flowering in rice. J. Plant Physiol. 168, 1837–1843.

Li, X.D., Xia, B., Wang, R., Xu, S., Jiang, Y.M., Yu, F.B., Peng, F., 2013c. Molecular cloning and characterization of S-adenosylmethionine synthetase gene from *Lycoris radiata*. Mol. Biol. Rep. 40, 1255–1263.

Lindroth, A.M., Saarikoski, P., Flygh, G.D., Gronroos, R., Thelander, Mattias, 2001. Two S-adenosylmethionine synthetase-encoding genes differentiallyexpressed during adventitious root development in *Pinus contorta*. Plant Mol. Biol. 46, 335–346.

Liu, W., Xie, Y., Ma, J., Luo, X., Nie, P., Zuo, Z., Lahrmann, U., Zhao, Q., Zheng, Y., Zhao, Y., 2015. IBS: an illustrator for the presentation and visualization of biological sequences. Bioinformatics 31, 3359–3361.

Livak, K.J., Schmittgen, T.D., 2001. Analysis of relative gene expression data using real-time quantitative PCR and the $2_{T}^{-\Delta\Delta C}$ method. Methods 25, 402–408.

Ma, C., Wang, Y., Gu, D., Nan, J., Chen, S., Li, H., 2017. Overexpression of S-adenosyl-L-methionine synthetase 2 from sugar beet M14 increased *Arabidopsis* tolerance to salt and oxidative stress. Int. J. Mol. Sci. 18, 847.

Maehly, A.C., Chance, B., 1955. The assay of catalases and peroxidases. Methods Enzymol. 2, 764–775.

Mao, D., Yu, F., Li, J., Van de Poel, B., Tan, D., Li, J., Liu, Y., Li, X., Dong, M., Chen, L., Li, D., Luan, S., 2015. FERONIA receptor kinase interacts with S-adenosylmethionine synthetase and suppresses S-adenosylmethionine production and ethylene biosynthesis in *Arabidopsis*. Plant Cell Environ. 38, 2566–2574.

Markham, G.D., Pajares, M.A., 2009. Structure-function relationships in methionine adenosyltransferases. Cell. Mol. Life Sci. 66, 636–648.

Minocha, R., Majumdar, R., Minocha, S.C., 2014. Polyamines and abiotic stress in plants: a complex relationship. Front. Plant Sci. 5, 175.

Moschou, P.N., Delis, I.D., Paschalidis, K.A., Roubelakis-Angelakis, K.A., 2010. Transgenic tobacco plants overexpressing polyamine oxidase are not able to cope with oxidative burst generated by abiotic factors. Physiol. Plantarum 133, 140–156.

Moschou, P.N., Paschalidis, K.A., Delis, I.D., Andriopoulou, A.H., Lagiotis, G.D., Yakoumakis, D.I., Roubelakisangelakis, K.A., 2008. Spermidine exodus and oxidation in the apoplast induced by abiotic stress is responsible for H_2O_2 signatures that direct tolerance responses in tobacco. Plant Cell 20, 1708–1724.

Moschou, P.N., Roubelakisangelakis, K.A., 2014. Polyamines and programmed cell death. J. Exp. Bot. 65, 1285–1296.

Nakano, Y., Asada, K., 1981. Hydrogen peroxide is scavenged by ascorbate-specific peroxidase in spinach chloroplasts. Plant Cell Physiol. 22, 867–880.

Peleman, J., Saito, K., Cottyn, B., Engler, G., Seurinck, J., Van Montagu, M., Inzé, D., 1989. Structure and expression analyses of the S-adenosylmethionine synthetase gene family in *Arabidopsis thaliana*. Gene 84, 359–369.

Pulla, R.K., Kim, Y.J., Parvin, S., Shim, J.S., Lee, J.H., Kim, Y.J., In, J.G., Senthil, K.S., Yang, D.C., 2009. Isolation of S-adenosyl-L-methionine synthetase gene from *Panax ginseng* C.A. meyer and analysis of its response to abiotic stresses. Physiol. Mol. Biol. Plants 15, 267–275.

Qi, Y.C., Wang, F.F., Zhang, H., Liu, W.Q., 2010. Overexpression of *suadea salsa* S -adenosylmethionine synthetase gene promotes salt tolerance in transgenic tobacco. Acta Physiol. Plant. 32, 263–269.

Quan, J., Zhang, S., Zhang, C., Meng, S., Zhao, Z., Xu, X., 2014. Molecular cloning, characterization and expression analysis of the *SAMS* gene during adventitious root development in IBA-induced tetraploid black locust. PLoS One 9, e108709.

Roeder, S., Dreschler, K., Wirtz, M., Cristescu, S.M., van Harren, F.J., Hell, R., Piechulla, B., 2009. SAM levels, gene expression of *SAM* synthetase, methionine synthase and ACC oxidase, and ethylene emission from *N. suaveolens* flowers. Plant Mol. Biol. 70, 535–546.

Roje, S., 2006. S-adenosyl-L-methionine: beyond the universal methyl group donor. Phytochemistry 67, 1686–1698.

Saitou, N., 1987. The neighbor-joining method : a new method for reconstructing phylogenetic tree. Mol. Biol. Evol. 4, 406–425.

Sanchez-Aguayo, I., Rodriguez-Galan, J.M., Garcia, R., Torreblanca, J., Pardo, J.M., 2004. Salt stress enhances xylem development and expression of S-adenosyl-L-methionine synthase in lignifying tissues of tomato plants. Planta 220, 278–285.

Shen, B., Li, C., Tarczynski, M.C., 2002. High free-methionine and decreased lignin content result from a mutation in the *Arabidopsis* S-adenosyl-L-methionine synthetase 3 gene. Plant J. 29, 371–380.

Shu, S., Chen, L., Lu, W., Sun, J., Guo, S., Yuan, Y., Li, J., 2014. Effects of exogenous spermidine on photosynthetic capacity and expression of Calvin cycle genes in salt-stressed cucumber seedlings. J. Plant Res. 127, 763–773.

Vandenbussche, F., Vaseva, I., Vissenberg, K., Van Der Straeten, D., 2012. Ethylene in vegetative development: a tale with a riddle. New Phytol. 194, 895–909.

Wang, K.L.C., Li, H., Ecker, J.R., 2002. Ethylene biosynthesis and signaling networks. Plant Cell 14, S131–S151.

Wang, L.W., He, M.W., Guo, S.R., Zhong, M., Shu, S., Sun, J., 2017. NaCl stress induces

CsSAMs gene expression in *Cucumis sativus* by mediating the binding of *CsGT-3b* to the GT-1 element within the *CsSAMs* promoter. Planta 245, 889–908.

Wang, W., Liu, J.H., 2016. *CsPAO4* of *Citrus sinensis* functions in polyamine terminal catabolism and inhibits plant growth under salt stress. Sci. Rep. 6, 31384.

Wang, X., Oh, M.W., Komatsu, S., 2016. Characterization of S-adenosylmethionine synthetases in soybean under flooding and drought stresses. Biol. Plant. 60, 269–278.

Wu, J., Shu, S., Li, C., Sun, J., Guo, S.J., 2018. Spermidine-mediated hydrogen peroxide signaling enhances the antioxidant capacity of salt-stressed cucumber roots. Plant Physiol. Biochem. 128, 152–162.

Yoda, H., Hiroi, Y., Sano, H., 2006. Polyamine oxidase is one of the key elements for oxidative burst to induce programmed cell death in tobacco cultured cells. Plant Physiol. 142, 193–206.

Yu, J.G., Lee, G.H., Park, Y.D., 2012. Physiological role of endogenous S-adenosyl-L-methionine synthetase in *Chinese cabbage*. Hort. Environ. Biotechnol. 53, 247–255.

Yuan, R.N., Shu, S., Guo, S.R., Sun, J., Wu, J.Q., 2017. The positive roles of exogenous putrescine on chlorophyll metabolism and xanthophyll cycle in salt-stressed cucumber seedlings. Photosynthetica 56, 557–566.

Yuan, Y., Zhong, M., Shu, S., Du, N., Sun, J., Guo, S., 2016. Proteomic and physiological analyses reveal putrescine responses in roots of cucumber stressed by NaCl. Front. Plant Sci. 7, 1035.

Zhang, R.H., Li, J., Guo, S.R., Tezuka, T., 2009. Effects of exogenous putrescine on gas-exchange characteristics and chlorophyll fluorescence of NaCl-stressed cucumber seedlings. Photosynth. Res. 100, 155–162.